International Journal of Fatigue 62 (2014) 210–216

Contents lists available at ScienceDirect

International Journal of Fatigue

journal homepage: www.elsevier.com/locate/ijfatigue

Effects of precipitated phases on the crack propagation behaviour of a Ni-based superalloy

Lei Wang [a,*], Shuai Wang [a], Xiu Song [a], Yang Liu [a], Guohua Xu [b]

[a] Key Laboratory for Anisotropy and Texture of Materials, Northeastern University, China
[b] High Temperature Materials Research Institute, Central Iron and Steel Research Institute, China

ARTICLE INFO

Article history:
Received 9 October 2012
Received in revised form 4 February 2013
Accepted 10 October 2013
Available online 18 October 2013

Keywords:
Nickel-based superalloys
Crack propagation behaviour
TCP phases
γ′ phase

ABSTRACT

Fatigue crack growth rate tests were carried out on a nickel-based superalloy GH4586 (in Chinese series) with various aging treatments at room temperature, to investigate the effect of precipitated phases on the crack propagation behaviour. The results show that the topologically close packed (TCP) phases precipitate and the γ′ phase and carbides at grain boundaries are coarsened after long time aging. The size of TCP phases becomes larger and the volume fraction of these phases increases with the increasing of aging time. The fatigue crack growth rate of the alloy at 700 °C for 500 h can be reduced by the small amount of TCP phases and coarsened γ′ phase with low coarsening degree, but it increases if these secondary phases are with large size and volume fraction. Very small quantity of TCP phases and small size γ′ phase in the alloy at 700 °C for 500 h can be cut through by dislocations, contributing to the yielding strength, thus the crack growth rate is reduced. Furthermore, cut-able TCP phases and γ′ phase leads to the formation of serrated and tortuous fracture surface, resulting in remarkable closure effect. On the other hand, the increasing of TCP phases and coarsened γ′ phase leads to the weakening of the crack closure effect and crack tip stress shielding effect.

1. Introduction

A new wrought Ni-based superalloy without the addition of noble metal elements such as Ta and Hf has been developed for gas turbine engine discs in China, which is named GH4586 in Chinese series [1]. It is strengthened by solid solution, precipitation of γ′ phase and carbides [2,3]. Since the superalloy exhibits satisfactory mechanical properties up to 650 °C [4,5], it has been widely used for aerospace applications.

In the past, although the effects of grain size, precipitation of γ′ phase, temperature, stress ratio and frequency on fatigue crack growth rate were studied by Xie [6], attention has been focused on the short-time mechanical properties, such as impact toughness, tensile deformation behaviour, high temperature stress rupture and creep properties. However, when the superalloy is used for aviation applications, the microstructure characteristics will be changed due to the long-term heating at high temperatures. Especially, unfavorable phase precipitated and the coarsening of strengthening phases during long-term high temperature. It is well known that the mechanical properties of a superalloy are influenced by the characteristics, size and morphology of precipitates. After long time exposure, the precipitates often lead to degradation of a superalloy [7–15]. Therefore, properties related to long duration should be taken into account and the effects of precipitated phases on the crack propagation behaviour are required to be explored.

In the present study, the fatigue crack growth rate tests were carried out on a Ni-based superalloy with various aging treatments at room temperature. The microstructure and the fatigue crack behaviour were observed and discussed. It is expected to provide fundamental data for the fatigue life prediction of the superalloy.

2. Material and experimental procedures

The material used in this study were prepared by vacuum induction melting and vacuum arc remelting, and then hot forged into Φ540 mm disc. The chemical composition of the alloy is shown in Table 1. The alloy was firstly treated by standard heat treatment consisting of solid solution at 1080 °C for 4 h followed by air cooling and aging at 760 °C for 16 h followed by air cooling. Material in this condition is marked as ST. Further, blanks cut from the ST material were long-term aged at 700 °C for 500 h, 1000 h and 1500 h, respectively. The microstructures of these alloys after different heat treatment were observed using LEXT 3000 confocal laser scanning microscope(CLSM) and JEOL 7001 field-emission scanning electron microscope (FE-SEM). The samples were

* Corresponding author. Address: Key Laboratory for Anisotropy and Texture of Materials, Northeastern University, 3-11 Wenhua road, Heping district, Shenyang 110819, China. Tel.: +86 24 83681685; fax: +86 24 23906316.
E-mail address: wanglei@mail.neu.edu.cn (L. Wang).

0142-1123/$ - see front matter © 2013 Elsevier Ltd. All rights reserved.
http://dx.doi.org/10.1016/j.ijfatigue.2013.10.006

Table 1
Chemical compositions of the Ni-based supperalloy (mass%).

Cr	Co	Mo	W	Al	Ti	Fe	C	B	Mg	Ni
19.09	10.68	8.11	3.05	1.61	3.18	0.100	0.050	0.003	0.003	Bal.

mechanically polished and then chemically etched in a solution of HCl (40 mL) + CH_3CH_2OH (20 mL)+$CuSO_4$ (1.5 g).

Fatigue crack growth rate tests were conducted in air at room temperature on a computer-controlled MTS 810 servohydraulic testing system. The Compact tension (CT) samples for FCGR were machined in the R–C orientation i.e. keeping the radial direction perpendicular to the notch plane and the crack propagation direction along the tangential direction. The sample dimensions were according to the ASTM standard with the width 'W' = 40 mm, thickness 'B' = 10 mm and notch length 'a_n' = 8 mm, as shown in Fig. 1. And 3 samples at each condition were tested. The samples were subjected to fatigue loading at 10 Hz to obtain a pre-crack length of 2 mm. The samples were cycled under stress intensity K control at a frequency of 3.3 Hz (sine wave) and a load ratio ($R = P_{min}/P_{max}$) of 0.1. Fatigue crack growth rate tests were performed initially under a K-decreasing procedure, with the normalized stress intensity gradient $C = (1/K)(dK/da)$ set to be $-0.1\ mm^{-1}$, and then under K-increasing procedure with $C = 0.1\ mm^{-1}$. Crack lengths were measured by the compliance method. Crack closure measurements were carried out by the linear/quadratic spline method. Crack growth rates were calculated by the seven-point polynomial technique, accordance with standard ASTM E647. The fatigue crack propagation paths were also observed by LEXT 3000 CLSM, and the fracture surfaces were analyzed by JEOL 7001 FE-SEM.

3. Results and discussion

3.1. Microstructure and precipitated phases

The microstructures of the alloy with different heat treatment are shown in Fig. 2. The microstructure of the alloy after standard heat treatment is composed of equiaxed grains with carbides distributed along grain boundaries and inside grains. The dispersive carbides along grain boundaries are mainly $M_{23}C_6$ type while the carbides inside grains are mainly M_6C type. It seems that there is no obvious change in the carbides inside grains after long-term aging, while long needle-like TCP phases precipitate. In addition, only a very small quantity of TCP phases are found aged at 700 °C for 500 h, as shown in Fig. 2(b) and the size and volume fraction of TCP phases of TCP phases increases with the increasing of the aging time. It has been confirmed that the TCP phases are mainly μ and σ phases [16,17].

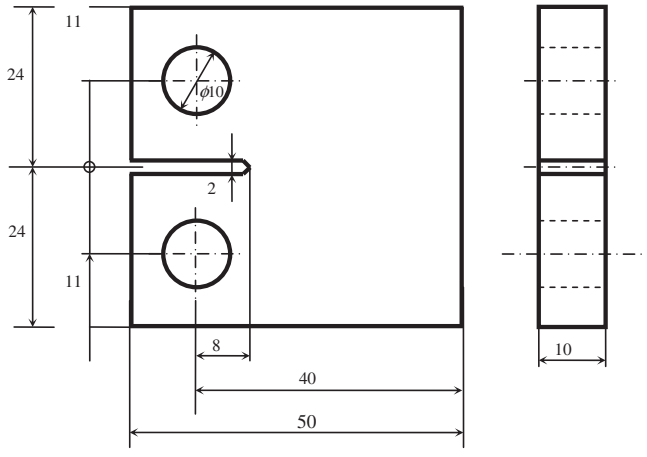

Fig. 1. Geometries of standard CT specimens for fatigue crack growth rate testing.

The SEM morphologies of the alloys with different aging time were shown in Fig. 3. It illustrates that the carbides along grain boundaries which are $M_{23}C_6$ are coarsened with the increasing of the aging time. While the quantity of grain boundary carbides is less than 0.5 wt%. Furthermore, the TCP phases are clearly seen near the $M_{23}C_6$. $M_{23}C_6$ on the grain boundaries, which can be as the nucleus of the TCP phases and then TCP phases grow into the grain. The high-magnification SEM morphologies of the alloys with different aging time are shown in Fig. 3(b, d, f, h). The γ′ phase size increases with the increasing of aging time. The size of γ′ phase is 33.4, 50.6, 63.2, 84.3 nm in the ST samples, 700 °C/500 h samples, 700 °C/1000 h samples, and 700 °C/1500 h samples, respectively. However, the quantity of γ′ phase is not influenced by long-term aging, keeping about 31 wt%.

3.2. Fatigue crack growth rate

The fatigue crack growth rate da/dN as a function of the nominally applied stress intensity factor range ΔK of the alloy with different aging time is plotted in Fig. 4. One typical curve at each condition were chosen in Fig. 4, because the data of the 3 tests at each condition are perform the same trend, and the differences between the data for different samples are within the small error range. As results showed above, the size and quantity of precipitates increase with the aging time, thus it could be illustrated that the fatigue crack growth rate increases with the increase in size and quantity of the precipitates.

For fatigue crack growth at stage I, ΔK_{th} of the testing alloy can be determined from the plots. The ΔK_{th} values correspond to a limiting crack growth rate of 10^{-9} m/cycle are listed in Table 2. Aged at 700 °C for 500 h is named as 700 °C/500 h. Other long-term aging treatments are also marked with the same way. It is noticed that the 700 °C/500 h sample has the highest value of ΔK_{th}, that means crack growth resistance in the near-threshold regime can be enhanced by the small amount of precipitates phases including TCP phases, coarsened γ′ phase or carbides. While the ΔK_{th} decreases in the alloy with the increasing quantity of TCP phases and coarsened γ′ phase or carbides.

The linear region of the plots of da/dN versus ΔK in Fig. 4 is found to obey the Paris Law given by: $da/dN = C(\Delta K)^n$, where the coefficient 'C' and the exponent 'n' are the Paris constants. The Paris constants determined from linear least squares fit of the data in Fig. 4 within the da/dN range from 2×10^{-8} to 4×10^{-7} m/cycle are shown in Table 2. It is obvious that the value of 'n' increases with increasing of aging time, while the value of 'C' does not change monotonically with aging time, indicating the complicated effect of aging-induced microstructure changes.

3.3. Fractographic characteristics

Fractographs of the alloy with different aging time at the fatigue crack growth rate of 2×10^{-8} m/cycle are shown in Fig. 5. The fracture feature of the samples is transgrainular. A typical feature of the ST, 700 °C/500 h and 700 °C/1000 h samples is the smooth crystallographic facets with fatigue striations. However, the